Appl. Phys. A (2016)122:1001
DOI 10.1007/s00339-016-0540-7

Applied Physics A
Materials Science & Processing

Internal modification of intrinsic and doped silicon using infrared nanosecond laser

Xiaoming Yu[1] · Xinya Wang[1] · Margaux Chanal[2] · Carlos A. Trallero-Herrero[3] · David Grojo[2] · Shuting Lei[1]

Received: 11 March 2016 / Accepted: 31 October 2016

Abstract We report experimental results of three-dimensional (3D) modification inside intrinsic and doped silicon wafers using laser pulses with 1.55 μm wavelength and 3.5 ns pulse duration. Permanent modification in the form of lines is generated inside silicon by tightly focusing and continuously scanning the laser beam inside samples, without introducing surface damage. Cross sections of these lines are observed after cleaving the samples and are further analyzed after mechanical polishing followed by chemical etching. With the objective lens corrected for spherical aberration, tight focusing inside silicon is achieved and the optimal focal depth is identified. The laser-induced modification has triangular shape and appears in regions prior to the geometrical focus, indicating significant absorption in those regions. Experiments with doped samples show similar modification for doping concentrations (and corresponding initial free carrier densities) in the range of 10^{13}–10^{16} cm^{-3}. At carrier densities of 10^{18} cm^{-3}, linear absorption of light becomes significant and the modification is reduced in size.

✉ Shuting Lei
lei@ksu.edu

[1] Department of Industrial and Manufacturing Systems Engineering, Kansas State University, Manhattan, KS 66506, USA

[2] CNRS, LP3 UMR 7341, Aix-Marseille University, 13288 Marseille, France

[3] J. R. Macdonald Laboratory, Department of Physics, Kansas State University, Manhattan, KS 66506, USA

1 Introduction

The ability to directly generate three-dimensional (3D) structures inside materials distinguishes laser-based materials processing from other planar lithographic methods and has been extensively studied for large-bandgap materials [1]. Potential applications with this 3D technique include the fabrication of optical waveguides [2], microfluidic network [3, 4], electronic circuits [5], and the integration of these components to realize lab-on-a-chip [6]. Fabrication in 3D is realized by concentrating large amount of laser energy within a small volume inside materials and is usually initiated through nonlinear processes such as multiphoton and avalanche ionization [7, 8]. Due to their large bandgaps, dielectric materials can be processed with laser wavelengths as short as in the ultraviolet range [9]. For example, formation of voids [10] and nano-channels [11] inside dielectrics has been reported.

Current semiconductor manufacturing processes, notably photolithography, are inherently planar methods, and 3D structures are achieved in a layer-by-layer fashion, which involves multiple steps and therefore increases defect rate and reduces yield. Laser-based 3D fabrication provides a one-step manufacturing solution and has the potential to reduce processing time and cost. To date, a wealth of knowledge about internal modification inside dielectrics has been gained and would be invaluable for applying this technique to other materials. Therefore, our goal is to extend such manufacturing techniques to semiconductors since semiconductors (such as silicon) form the basis of modern electronics. The reader can refer to Ref. [12] for a short review on internal modification of silicon. Recent advances include internal modification for wafer dicing [12], double-femtosecond-laser-pulse-induced modification [13], machining on the back surface of silicon

Published online: 07 November 2016

[14], and an attempt to fabricate microchannels inside silicon [15].

However, 3D processing of semiconductors is a relatively new topic, and some critical issues related specifically to it need to be addressed. First, due to the large difference of refractive indices between air ($n = 1$) and silicon ($n = 3.5$), more severe spherical aberration (SA) is expected for focusing in silicon than in glass ($n \sim 1.5$), especially with high numerical aperture (NA) optics. SA should be corrected in order to achieve diffraction-limited focusing. Second, direct observation of internal structures inside semiconductors requires infrared optical microscopy, which is less commonly used than its visible-light counterpart and typically has lower resolution due to the use of longer-wavelength light. A commonly used destructive analysis method is cleaving samples and then observing cross sections with visible-light or scanning electron microscopy. For this method to be accurate, it is necessary to distinguish between modification/damage induced solely by the laser and that introduced by the cleaving procedure, as has been pointed out by others [12]. Third, the order of multiphoton ionization (m) for dielectrics and near-infrared lasers is usually large ($m = 6$ for fused silica and 800 nm laser wavelength), and therefore absorption can be confined in a small volume around the geometrical focus. For silicon (with a bandgap of 1.1 eV) and lasers with wavelengths in the telecommunication range (around 1.5 μm, photon energy 0.8 eV), m is only 2, resulting in weaker confinement and larger absorption volume. It is therefore necessary to investigate the maximum energy density achieved at the focus, a key parameter determining whether or not significant damage can be generated [10].

In this paper, we attempt to address these issues by investigating the formation of modification inside intrinsic silicon wafers using a fiber laser with 1.55 μm wavelength and 3.5 ns pulse duration. By tightly focusing the laser beam with SA correction, we write continuous lines inside intrinsic silicon and doped silicon samples and analyze their cross sections. The absorption is found to occur before the laser beam reaches its optical geometrical focus, resulting in energy density orders-of-magnitude lower than that required to initiate significant damage. This work expands the ongoing research on 3D fabrication of dielectrics to semiconductor materials, with the objective aimed at realizing direct 3D processing of semiconductors using optimally designed laser beams.

2 Experimental details

The experimental setup is sketched in Fig. 1. The laser is a fiber MOPA (master oscillator power amplifier) laser (MW Technologies, Model PFL-1550) delivering laser pulses at

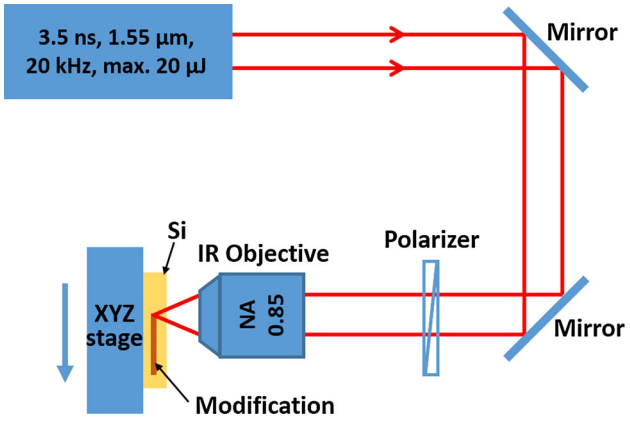

Fig. 1 Experimental setup. See text for details

1.55 μm center wavelength and 3.5 ns FWHM (full-width-at-half-maximum of the intensity) pulse duration. The repetition rate is tunable from 20 to 150 kHz and is fixed at 20 kHz in this study. The maximum pulse energy is 20 μJ. The output beam is collimated and has a $1/e^2$ diameter of 6 mm. Two metallic mirrors are used to route the beam. It should be noted that the polarization of the output beam is not determined by the manufacturer, and our measurements show an elliptical polarization at the output of the laser. A Glan–Taylor polarizer is used in the latter part of this study (Sect. 3.4) to allow only linear polarization to pass through. Laser power is adjusted directly on the control unit and measured before the objective lens. We compare this method of controlling laser power with the polarizer-halfwave plate-polarizer method [12] and find no noticeable difference in the final results. The beam is focused by a 0.85-NA infrared objective lens (Olympus, Model LCPLN100XIR), which has SA correction for silicon thickness of 0–1 mm. The input aperture size of the objective is 3.5 mm, resulting in ~50% energy loss due to clipping. The estimated focal spot diameter and confocal length inside silicon are 1.5 and 8 μm, respectively (shown below). The samples used in this study are (100)-oriented, 1-mm-thick silicon wafers, either intrinsic or n/Ph-doped. The intrinsic samples have a resistivity of >200 Ω cm and are used first in the experiment to find the best focal depth and reveal the damage morphology. Four n-doped samples, with resistivity of 50–100 Ω cm, 10–14 Ω cm, 0.5–0.8 Ω cm, and 0.015–0.025 Ω cm, are used in the latter part of the study to investigate the effect of doping. The wafers are cleaved into small pieces of about 20 × 20 mm^2, which are mounted on a motorized XYZ stage (Newport, Model ILS100PP). The focal depth is controlled by moving the sample along the laser beam's axial direction, and modification is induced by scanning the sample transversely at a constant speed of 1 mm/s. The focus overlapping is >97% at this speed. To ensure that the

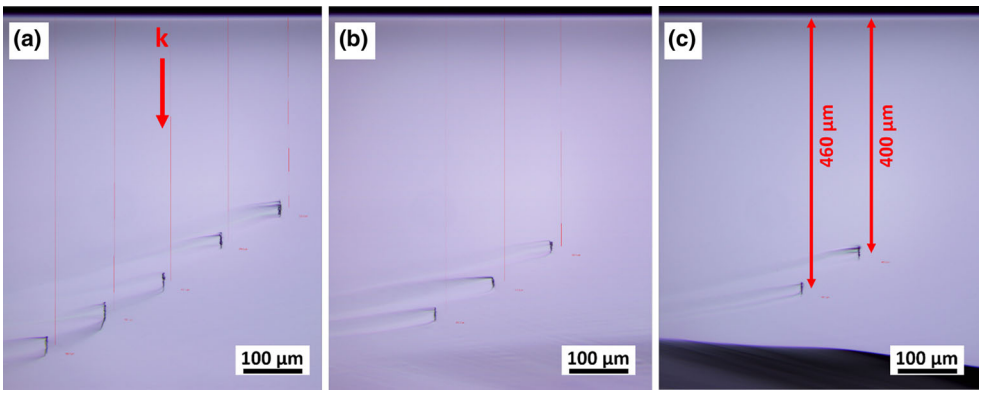

Fig. 2 Cross sections of modification lines in silicon at various depths with pulse energy (measured before the objective lens) of **a** 2.5 µJ, **b** 2 µJ, and **c** 1.5 µJ. Regions in *black* color and aligned vertically are laser-induced modification. Narrow *vertical lines* in *red* color are depth measurements

focal depth is constant during scanning, the position of the sample is carefully adjusted so that within the area of interest (typically 5×5 mm^2), the difference in focal depth is <50 µm. The focus on the front surface is determined when white plasma from surface damage is observed, and the desired depth (d) is reached by moving the sample toward the objective by d/n, where $n = 3.5$ is the refractive index of silicon at 1.55 µm. The sample after laser writing is cleaved perpendicularly to the scanning direction, and the cross sections (in the (110)-plane) are observed with a visible-light microscope. The cleaved surface is then gently polished and examined with the microscope again (no modification is observed, shown below). The polished surface is etched in a 50% wt KOH solution for 5 min (in an ultrasonic bath) to reveal the modified regions and observed with the microscope. In this study, damage is not observed on either front or back surface of the silicon samples. In this study, the term "modification" refers to any permanent change in the sample after laser treatment, and "damage" refers to significant modification, such as cracks and voids.

3 Results and discussion

3.1 Optimal focal depth with spherical aberration (SA) correction

Due to the large difference of refractive indices between air and silicon, spherical aberration is expected to be significant and needs to be compensated. The objective lens used in this study has a correction collar and can compensate aberration in silicon with thickness up to 1 mm, which is also the thickness of our samples. To facilitate later characterization of induced modification, we choose to generate modification in the middle of the samples, and therefore the correction collar is set at 0.5 mm throughout the experiments. It should be noted that setting the correction at 0.5 mm does not guarantee optimal focusing at this depth (shown below), since the lens might be designed around a wavelength different from our laser wavelength. To get this optimal focusing depth, we write continuous lines at various depths with 50 µm increments, at a constant speed of 1 mm/s. The samples are then cleaved perpendicularly to the writing direction, and the cross sections are examined with a visible-light microscope. The results for three pulse energies are shown in Fig. 2. Pulse energies in Fig. 2 and in all the following figures are measured before the objective lens, without taking into account energy loss at the objective aperture and air–Si interface. The polarizer is not used in obtaining Fig. 2. Regions in black color and aligned vertically are laser-induced modification, and the structures seen outside these regions are caused by the cleaving procedure. For a high pulse energy of 2.5 µJ, modification is observed within a wider depth range, from 350 to 550 µm. This range reduces for a lower energy of 1.5 µJ, and only two modifications at 400 and 460 µm can be observed. No modification is seen when the pulse energy is reduced to 1 µJ.

The results in Fig. 2 can be easily understood by calculating the focal shape at various depths, with the consideration of refractive index mismatch. To show this, we use the PSF Lab software [16] to obtain focal intensity profiles. The objective lens is assumed to be perfectly corrected for 430-µm-thick silicon, and intensities at various depths are calculated, as shown in Fig. 3. We can see that at the depth corresponding to the correction depth (430 µm), the focus is a diffraction-limited spot with size consistent with estimation (Fig. 3c). When the foci are shifted by about 50 µm (b and d), the foci are elongated and the peak intensities drop to about 70% of the peak intensity in (c). Further shifting the depth causes even longer foci and lower (35%) peak intensities. This shows that a shift in depth as small as 50 µm can cause reduction

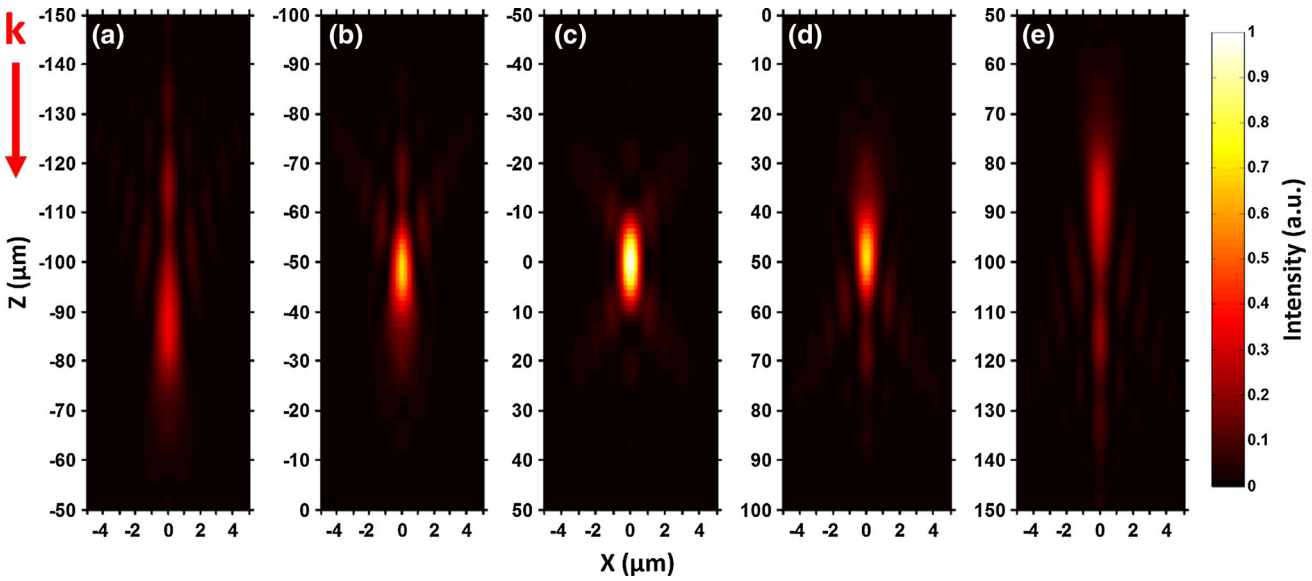

Fig. 3 Calculated focal intensities at various depths inside silicon with the consideration of refractive index mismatch. $Z = 0$ corresponds to a depth of 430 μm. The intended focal depths are $Z = -100$, -50, 0, 50 and 100 μm for (**a**–**e**), respectively. Intensities in all the images are normalized to the peak intensity in (**c**)

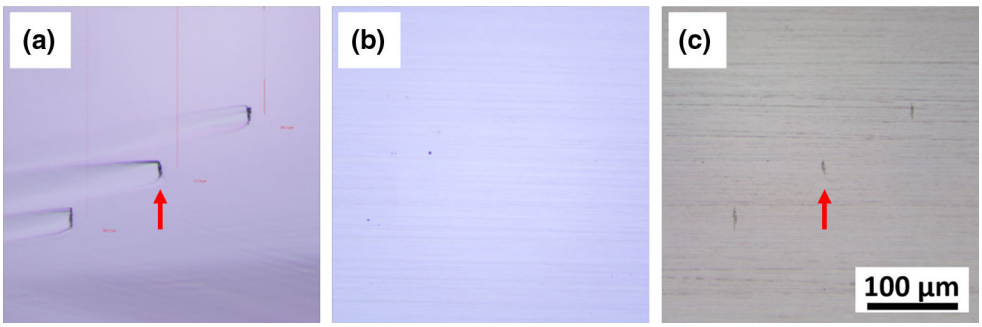

Fig. 4 Cross sections of laser-modified regions after **a** cleaving, **b** polishing, and **c** chemical etching. Two cross sections pointed by *arrows* are magnified in Fig. 5

in peak intensities and as a consequence disappearance of laser-induced modification, in consistence with the experimental results shown in Fig. 2. In the following experiments, the laser focus is positioned in the optimal depth range of 400–460 μm.

3.2 Observation of modification after polishing and KOH etching

Modification inside silicon can be observed nondestructively with infrared microscopy, which has been used by others [12–14]. In this study, we choose to observe the modification by cleaving the sample. This destructive method, however, induces undesired alteration to the samples (Fig. 2) that might be indistinguishable from the modification caused solely by the laser. To avoid confusion, we apply the polishing and etching method that is commonly used in the study for dielectrics [17] and has also been used for silicon recently [14]. The sample from the previous experiment (Fig. 2b, also shown in Fig. 4a) is mechanically polished, and the polished surface is examined under a visible-light microscope. Interestingly, the modified regions completely disappear after polishing, as shown in Fig. 4b. A similar behavior is also reported for femtosecond laser writing [13]. We verify that modification caused by the highest pulse energy (20 μJ) and a much slower scanning speed (0.01 mm/s) also disappears after polishing (results not shown here). These findings suggest that the laser-induced modification in this study might merely be local change of density [13], not significant damage such as cracks and voids, because otherwise one would expect to see some type of irregularities on the polished surface. The change of density manifests itself after the disturbance during the sample cleaving procedure, and therefore modified regions can be observed in Fig. 4a.

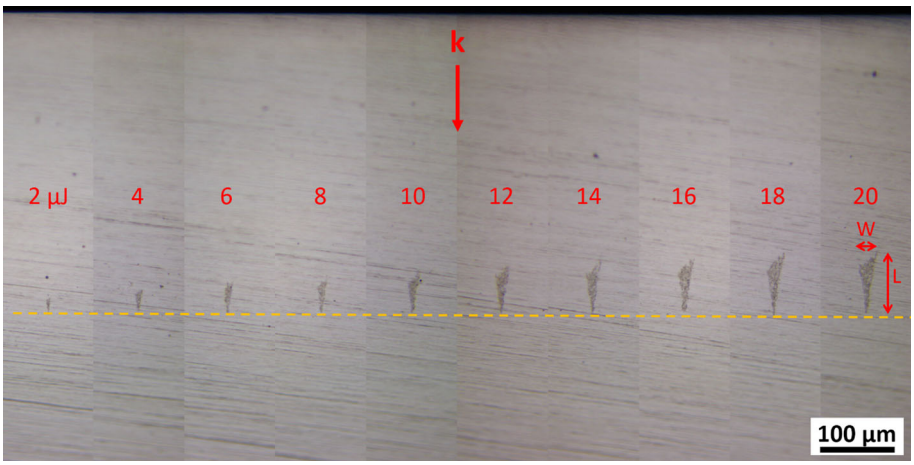

Fig. 5 Laser-induced modification at the same depth (400 μm) and with increasing pulse energy. The *horizontal dashed line* marks the focusing depth. Laser polarization is random. Width (*W*) and length (*L*) of modified region are measured as depicted. *Numbers* above modified regions represent pulse energy in μJ

To reveal the regions modified solely by the laser, the polished sample is etched by 50 wt% KOH solution for 5 min. The etching is facilitated in an ultrasonic bath. The same surface after etching is shown in Fig. 4c, and the laser-modified regions reappear. Meanwhile, the alteration caused by cleaving is absent. The etching selectivity may arise from mechanisms similar to those in dielectrics [6].

To shed light on the nature of laser-induced modification, we examine the surfaces shown in Fig. 4 using scanning electron microscopy (SEM) operating in the secondary electron mode (images not shown). We find that: (1) The cleaved surface (Fig. 4a) shows fractured structures within laser-modified regions, in consistence with previous studies [12]. (2) On the polished surface (Fig. 4b), while absent from optical images, the modified regions appear under SEM in a lighter color than the surrounding, pristine material. This is contrary to a previous study [13] where laser-modified region has a darker color and is believed to have lower density. Further analysis will be conducted to clarify this discrepancy. (3) After KOH etching (Fig. 4c), we observe a morphology similar to that observed in visible-light microscopy (shown below in Fig. 5), suggesting that the optical method used in this study is adequate in assessing the laser-modified regions.

3.3 Morphology of resultant modification

As mentioned above, absorption of 1.55 μm wavelength light in silicon is initiated by two-photon absorption, rather than the 6-photon process for 800 nm wavelength and fused silica. Therefore, the volume of absorbed energy is expected to be less confined than the latter case. The nature of absorption is further complicated by the small difference between the photon energy (0.8 eV) and the bandgap (1.1 eV), as it has been noted that the heating of silicon by the laser may cause the bandgap to shrink, leading to linear absorption [12]. It is therefore necessary to quantify the size and volume of absorption regions.

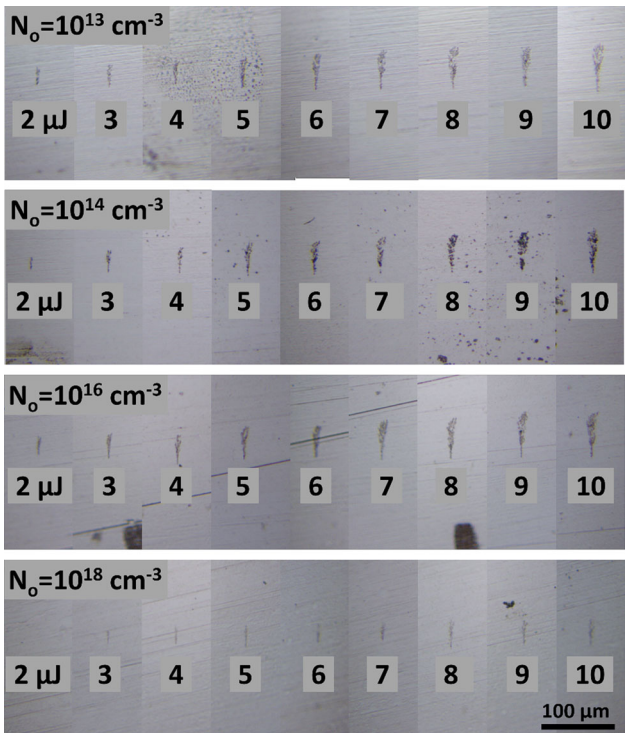

Fig. 6 Laser-induced modification in silicon wafers with various level of doping (free carrier density, N_o, indicated in the *top left* of each subfigure). Pulse energy is indicated on the bottom of each modification

To this end, we focus the beam at a fixed depth of 400 μm and write lines with increasing pulse energy. The cross sections treated after the polishing-etching procedure are shown in Fig. 6. The horizontal dashed line marks the intended focal depth of 400 μm. Although it is difficult to determine its exact depth, the focus should reside within or in the vicinity of the modification induced by the lowest pulse energy (2 μJ). The same focal depth is maintained

throughout this sample with an accuracy better than 20 μm. Larger modified regions are seen with increasing pulse energy, as would be expected. However, these regions enlarge asymmetrically, toward only the laser beam incoming direction. The modification from high pulse energies shows an inverse-triangle shape. These results suggest that the energy is absorbed in the regions before the geometric focus (on the plane marked by the dashed line). Since the maximum peak power delivered inside silicon is 2 kW, an order of magnitude below the critical power for self-focusing [12], collapse of the laser beam is not responsible for the increase in modification toward the laser beam. A simple estimate of total energy confined in the modified volume shows that the highest energy density can reach 4.6 kJ/cm^3 (with the consideration of energy loss at objective lens aperture and air–Si interface), high enough for silicon to reach the melting temperature (1687 K). However, the increased modification size with increasing pulse energy is undesired for localization of laser energy and high-precision laser processing. It is crucial to understand the fundamental mechanisms in the laser energy deposition process in order to realize 3D fabrication capabilities in semiconductors.

3.4 Effect of doping

In [18], it has been shown that localized nonlinear absorption can be achieved in doped silicon with free carrier density up to 10^{18} cm^{-3}. However, due to the increased linear absorption at high doping levels, laser energy reached at the focus is expected to decrease since light is absorbed before it reaches the focus. In this section, we investigate the effect of doping (free carrier density, N_0) on the resultant modification. Four samples with free carrier concentration of 10^{13}, 10^{14}, 10^{16}, and 10^{18} cm^{-3} are used. During the laser treatment, the focal depth is maintained at about 460 μm with an accuracy better than 20 μm among these samples, ensuring that the focus distortion due to spherical aberration (Fig. 3) is small. Other experiment conditions, such as scanning speed and the amount of time for chemical etching, are kept the same. Optical images of etched cross sections in doped silicon are shown in Fig. 6, and measured lengths and widths are shown in Fig. 7. Both of the figures show results as a function of doping and energy per pulse. Note that in obtaining Fig. 6, the polarizer is inserted to allow linear polarization (perpendicular to the scanning direction) to pass through. Results from the orthogonal linear polarization (parallel to the scanning direction) are similar to those in Fig. 6 and are not shown here.

From Fig. 6 we can see that, at each pulse energy, the shape of modified region is similar for $N_0 = 10^{13}$, 10^{14}, and 10^{16} cm^{-3}. Small differences in the shape and the contrast between the modified and surrounding regions are attributed to variations in the polishing and etching process. This observation is confirmed in Fig. 7, where the measured lengths and widths show a similar, linear relationship with the pulse energy. The similarity of resultant modification at lower dopant concentrations suggests an energy absorption mechanism independent of initial free carrier densities, in consistency with a previous study [18]. As N_0 increases to 10^{18}−cm^{-3}, we observe significant reduction in both modification size and contrast. While the lengths and widths also show a nearly linear relationship, the values are halved at each pulse energy compared to the other three samples. No modification is seen at 2 μJ pulse energy. This behavior can be understood if we take into account the appearance of linear absorption at high carrier densities of 10^{18} cm^{-3}. As has been shown previously [18], linear absorption becomes significant at this concentration. In fact, we find that the 50% reduction in length and width agrees quantitatively well with the amount of linear

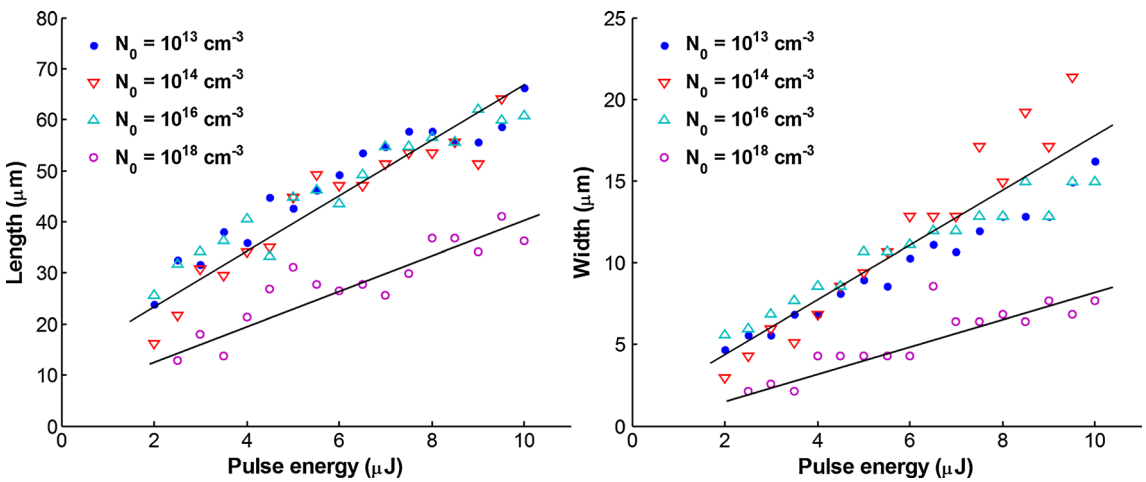

Fig. 7 Measured length and width of modified region at various doping levels. *Solid lines* are a guide to the eye

absorption ($\sim$40%) though a thickness of 500 μm (similar to the focal depth used in this study), assuming that length and width increase linearly with pulse energy.

4 Conclusion

In conclusion, we use a fiber laser with 1.55 μm wavelength and 3.5 ns pulse duration to generate permanent modification inside intrinsic and doped (change of carrier density) silicon wafers. Spherical aberration is found to be important and needs to be corrected for tight focusing at desired depth. While laser-induced modification can be clearly observed after cleaving the samples and exposing the cross sections, the modification disappears after mechanical polishing, suggesting the absence of severe damage such as cracks and voids. Increasing pulse energy causes the modified region to expand asymmetrically toward the incoming beam and therefore reduces the energy density deposited near the focal volume. This natural peak intensity "clamping" could be responsible for the lack of additional severe damage, even at high energy densities. Our studies on damage as a function of carrier density show that modifications are found to be independent on initial carrier density in the range of 10^{13}–10^{16} cm^{-3}. However, at a higher density of 10^{18} cm^{-3}, linear absorption of light before the focus reduces the pulse energy reached at the focus and thus the size of the induced modification. The change in modification dimensions is compatible with previous measurements of the linear absorption rate at the same carrier density.

Acknowledgements Finance support for the author C. T-H and laser support are provided by the Chemical Sciences, Geosciences, and Biosciences Division, Office of Basic Energy Sciences, Office of Science, US Department of Energy (DOE) under Grant No. DE-FG02-86ER13491. Partial financial support for this work by the National Science Foundation under Grant No. CMMI-1537846 is also gratefully acknowledged.

References

1. R. Gattass, E. Mazur, Femtosecond laser micromachining in transparent materials. Nat. Photonics **2**, 219–225 (2008)
2. K.M. Davis, K. Miura, N. Sugimoto, K. Hirao, Writing waveguides in glass with a femtosecond laser. Opt. Lett. **21**, 1729–1731 (1996)
3. K. Sugioka, Y. Hanada, K. Midorikawa, Three-dimensional femtosecond laser micromachining of photosensitive glass for biomicrochips. Laser Photonics Rev. **4**, 386–400 (2010)
4. Y. Liao, J. Song, E. Li, Y. Luo, Y. Shen, D. Chen et al., Rapid prototyping of three-dimensional microfluidic mixers in glass by femtosecond laser direct writing. Lab Chip **12**, 746–749 (2012)
5. J. Xu, Y. Liao, H. Zeng, Z. Zhou, H. Sun, J. Song et al., Selective metallization on insulator surfaces with femtosecond laser pulses. Opt. Express **15**, 12743–12748 (2007)
6. R. Osellame, H.J.W.M. Hoekstra, G. Cerullo, M. Pollnau, Femtosecond laser microstructuring: an enabling tool for optofluidic lab-on-chips. Laser Photonics Rev. **5**, 442–463 (2011)
7. E.G. Gamaly, A.V. Rode, Physics of ultra-short laser interaction with matter: from phonon excitation to ultimate transformations. Prog. Quantum Electron. **37**, 215–323 (2013)
8. P. Balling, J. Schou, Femtosecond-laser ablation dynamics of dielectrics: basics and applications for thin films. Rep. Prog. Phys. **76**, 036502 (2013)
9. X. Yu, Q. Bian, B. Zhao, Z. Chang, P.B. Corkum, S. Lei, Near-infrared femtosecond laser machining initiated by ultraviolet multiphoton ionization. Appl. Phys. Lett. **102**, 101111 (2013)
10. E.G. Gamaly, S. Juodkazis, K. Nishimura, H. Misawa, B. Luther, Davies, laser-matter interaction in the bulk of a transparent solid: confined microexplosion and void formation. Phys. Rev. B **73**, 214101 (2006)
11. Y. Liao, Y. Shen, L. Qiao, D. Chen, Y. Cheng, K. Sugioka et al., Femtosecond laser nanostructuring in porous glass with sub-50 nm feature sizes. Opt. Lett. **38**, 187–189 (2013)
12. P.C. Verburg, G.R.B.E. Römer, A.J. Huis in 't Veld, Two-photon–induced internal modification of silicon by erbium-doped fiber laser. Opt. Express **22**, 21958–21971 (2014)
13. M. Mori, Y. Shimotsuma, T. Sei, M. Sakakura, K. Miura, H. Udono, Tailoring thermoelectric properties of nanostructured crystal silicon fabricated by infrared femtosecond laser direct writing. Phys. Status Solidi **7**, 1–7 (2015)
14. Y. Ito, H. Sakashita, R. Suzuki, M. Uewada, K.P. Luong, R. Tanabe, Modification and machining on back surface of a silicon substrate by femtosecond laser pulses at 1552 nm. J. Laser Micro Nanoeng. **9**, 98–102 (2014)
15. D. Grojo, A. Mouskeftaras, P. Delaporte, S. Lei, Limitations to laser machining of silicon using femtosecond micro-Bessel beams in the infrared. J. Appl. Phys. **117**, 153105 (2015)
16. M.J. Nasse, J.C. Woehl, Realistic modeling of the illumination point spread function in confocal scanning optical microscopy. J. Opt. Soc. Am. A **27**, 295–302 (2010)
17. X. Yu, Y. Liao, F. He, B. Zeng, Y. Cheng, Z. Xu et al., Tuning etch selectivity of fused silica irradiated by femtosecond laser pulses by controlling polarization of the writing pulses. J. Appl. Phys. **109**, 053114 (2011)
18. S. Leyder, D. Grojo, P. Delaporte, W. Marine, M. Sentis, O. Utéza, Non-linear absorption of focused femtosecond laser pulses at 1.3 μm inside silicon: independence on doping concentration. Appl. Surf. Sci. **278**, 13–18 (2013)